Bioinspired polymeric heart valves: A combined in vitro and in silico approach

Check for updates

Aeryne Lee, PhD,[a,b] Xinying Liu, PhD,[a] Jacopo Emilio Giaretta, PhD,[a] Thanh Phuong Hoang,[a] Matthew Crago, BE,[a] Syamak Farajikhah, PhD,[a,c] Luke Mosse, PhD,[d] David Frederick Fletcher, PhD,[a] Fariba Dehghani, PhD,[a,c] David Scott Winlaw, MD,[b,e] and Sina Naficy, PhD[a,b,c]

ABSTRACT

Background: Polymeric heart valves (PHVs) may address the limitations of mechanical and tissue valves in the treatment of valvular heart disease. In this study, a bioinspired valve was designed, assessed in silico, and validated by an in vitro model to develop a valve with optimum function for pediatric applications.

Methods: A bioinspired heart valve was created computationally with leaflet curvature derived from native valve anatomies. A valve diameter of 18 mm was chosen to approach sizes suitable for younger patients. Valves of different thicknesses were fabricated via dip-coating with siloxane-based polyurethane and tested in a pulse duplicator for their hydrodynamic function. The same valves were tested computationally using an arbitrary Lagrangian–Eulerian plus immersed solid approach, in which the fluid–structure interaction between the valves and fluid passing through them was studied and compared with experimental data.

Results: Computational analysis showed that valves of 110 to 200 μm thickness had effective orifice areas (EOAs) of 1.20 to 1.30 cm², with thinner valves exhibiting larger openings. In vitro tests demonstrated that PHVs of similar thickness had EOAs of 1.05 to 1.35 cm² and regurgitant fractions (RFs) <7%. Valves with thinner leaflets exhibited optimal systolic performance, whereas thicker valves had lower RFs.

Conclusions: Bioinspired PHVs demonstrated good hydrodynamic performance that exceeded ISO 5840-2 standards. Both methods of analysis showed similar correlations between leaflet thickness and valve systolic function. Further development of this PHV may lead to enhanced durability and thus a more reliable heart valve replacement than contemporary options. (JTCVS Open 2023;15:113-24)
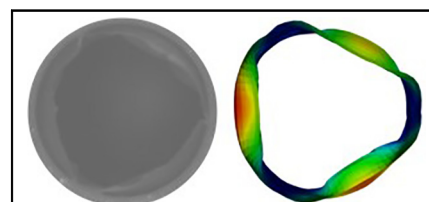
Bioinspired heart valve systolic performance: polymeric construct versus computational model.

CENTRAL MESSAGE

A bioinspired valve geometry was created using computer-aided design software and tested for its valvular performance both computationally and experimentally via pulse duplicator technology.

PERSPECTIVE

A novel valve design incorporating bioinspired leaflet curvatures demonstrated hydrodynamic performance that met the conditions set by the ISO 5840 standards. Computer simulation was able to successfully capture valve behavior under systole. In the future, full fluid–structure interaction analysis, in addition to optimization of fabrication processes, could lead to a polymeric heart valve with enhanced performance and durability.

https://doi.org/10.1016/j.xjon.2023.06.020

▶ Video clip is available online.

To view the AATS Annual Meeting Webcast, see the URL next to the webcast thumbnail.

Heart valve diseases and defects affect both children and adults, leading to approximately 300,000 valve replacements performed annually worldwide.[1] Many congenital heart diseases often require intervention in the right ventricular outflow tract.[2] Current treatment modalities include mechanical, bioprosthetic, and homograft valves. Although they can restore valve function, these replacement valves become dysfunctional over time and typically fail within 15 to 20 years of implantation.[3-10]

The main concern with mechanical valves is the high risk of thrombosis, which necessitates the lifelong use of anticoagulants. Although bioprosthetic valves have demonstrated hemodynamic flows comparable to native valves and fewer thrombogenic events than mechanical valves, they may trigger immune responses that accelerate structural valve deterioration. The main drawbacks of homograft are limited donor supply and availability of smaller sizes. For all valve types, structural valve deterioration and somatic outgrowth lead to the need for repeated valve procedures in pediatric patients.[11]

Although they have been the subject of research since the 1950s, polymeric heart valves (PHVs) have recently demonstrated clinical potential. Early outcomes in adult aortic valve replacement showed satisfactory hemodynamic performance, although further clinical studies are needed to assess long-term biostability and biocompatibility.[12]

The aim of the present work was to develop a PHV with optimized geometry to improve its hydrodynamic function by increasing the effective orifice area (EOA) and

comparing the performance of valves with different leaflet thicknesses. This study is a continuation of our previously developed bioinspired valve design, in which we used computed tomography scan images of native pulmonary valves to derive geometries based on the native valve.[13] In the present study, the valves were downsized from 30 mm (adult) to 18 mm (pediatric) in diameter to test their performance in the pulmonary position and the suitability for pediatric patients. The geometry of leaflet free edges was improved to minimize commissural gaps. In addition, a fluid–structure interaction (FSI) simulation was performed using an arbitrary Lagrangian-Eulerian (ALE) coupled to an immersed solid approach instead of conducting a structural analysis alone which was shown in our previous work.[13] This allowed us to account for the impact of the fluid motion and calculate the EOA in silico. In the FSI simulation, the performance of bioinspired valves was assessed for systolic function and stress distribution. PHV prototypes were fabricated with the same design using polyurethane and tested in a pulse duplicator system to evaluate their hydrodynamic performance and compare their opening behavior with results predicted in silico.

METHODS

Bioinspired Valve Design

A bioinspired valve geometry was developed as described previously based on a micro-CT scanned sheep valve.[13] The sheep valve was selected for use in this study because its anatomy is relatively similar to the human valve, and also because it can be readily sourced from a local butcher. In brief, to create a leaflet geometry emulating the natural curvature of native valves, one curve lying longitudinally through the middle of the leaflet surface was extracted. This curve was defined using a third-order polynomial function. Three copies of this curve were produced and lofted together (with surfaces built between chosen edges) to produce a single leaflet geometry.

This single leaflet was rotated about the central axis of the valve to form a trileaflet valve. Owing to the curved leaflet shape, the outcome was a valve with overlapping cusps, as shown in Figure 1, *B*. In the previous method, this was addressed by pulling the leaflets away from one another with respect to the central axis until they were no longer overlapping. This inevitably generated larger gaps at the free edge (Figure 1, *C*). Although this geometry performed very well computationally during systole, additional in silico and in vitro studies assessing closing performance suggested that gaps at the commissures could be minimized to reduce regurgitation and thereby optimize function.

In the new and improved design, a line was drawn from the commissure to the center of the valve between each leaflet (indicated in green in Figure 1, *D*). The free edge was redefined based on these 3 lines. Each leaflet geometry was relofted with the newly constructed lines in addition to the 3 existing third-order polynomial-based curves. The resulting surface had sharp changes in curvature on the leaflet surface, however (Figure 1, *E*), and thus required filleting to achieve a smoother leaflet curvature (Figure 1, *F*). The resulting valve (shown in Figure 1, *G*) was then tested for its hydrodynamic performance via in vitro and in silico approaches.

Hydrodynamic Testing

PHV prototypes were produced by dip-coating. In brief, molds based on the design described above were 3D-printed (Flashforge Adventurer 4 3D printer) using a polypropylene filament. The molds were then manually dip-coated in a siloxane-based polyurethane (PSU; Chronosil 85A,

AdvanceSource Biomaterials) dissolved in tetrahydrofuran. PSU was selected because of its ease of manufacture, favorable mechanical properties, and potential improvements in biological properties compared with other polymers, such as polytetrafluoroethylene.[14,15] The parameters of the dip-coating process, such as the temperature and the immersion time, were optimized to improve the homogeneity of the leaflet thickness and reduce bubble formation. The coated molds were then inverted (with the outflow surface of the leaflets pointing downward) to dry before the coating was removed and the top orifice was opened with a surgical blade, obtaining 18-mm diameter valves (Figure 2, A). Different leaflet thicknesses were achieved by changing the PSU concentration, within a range of 11 to 15 weight per volume percent (w/v%), which was identified as the manufacturing limits of the solution. The thickness of the valves was measured in different locations of the leaflet (Figure 2, B). Thickness was recorded for all leaflets in 3 different valves for each concentration tested, for a total of 9 data points per concentration.

Seven PHVs were hydrodynamically tested in the pulse duplicator system (HDTi-6000; BDC Labs) following ISO 5840 criteria and conditions of analysis. The formulas used to calculate the performance indicators, such as effective orifice area (EOA) and regurgitant fraction (RF), were obtained from this standard. Other valve assessments, including corrosion, accelerated wear testing, thrombogenic and hemolytic potential,

and fatigue, were beyond the scope of this study. The valves were fixed into a 3D-printed rigid holder (polylactic acid) before being mounted into the equipment. All tests were conducted under normotensive conditions in the pulmonary valve position with a simulated cardiac output of 5 L min^{-1}, heart rate of 70 bpm, 35% systolic duration, and 15 mm Hg mean arterial pressure for a total of 10 cycles per valve. The test fluid was isotonic saline (0.9 w/v% sodium chloride) with the system temperature was set to 37 °C. The 3 hydrodynamic parameters used for evaluation of valves were EOA, RF, and mean positive pressure gradient (PPD), calculated using the equipment software.

The pressure difference (ΔP) across the valve is defined as the difference between the ventricular and arterial pressure (ie, inlet pressure – outlet pressure). The mean PPD is calculated from the ΔP occurring over the time period when the inlet pressure is greater than the outlet pressure,

$$\text{Mean PPD (mmHg)} = \frac{\int_{t_s}^{t_e} (P_i(t) - P_o(t))\,\mathrm{d}t}{(t_e - t_s)},$$

where P_i and P_o denote the inlet and outlet pressures, respectively, and t_s and t_e are the times at the start and end, respectively, of the period when the inlet pressure exceeds the outlet pressure.
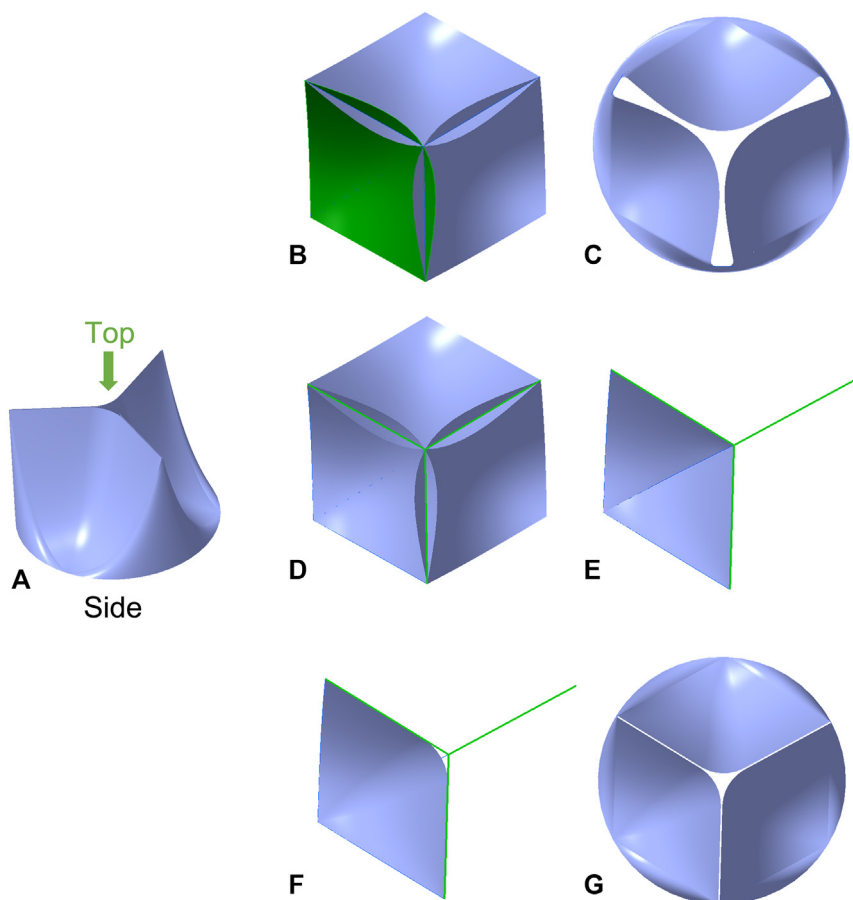

FIGURE 1. Step-by-step diagram showing the design process of the bioinspired valve design with minimized commissural gaps. A, Side view of the valve; the *green arrow* indicates top view of the valve where the following steps are illustrated. B, Tri-leaflet valve developed from rotating the highlighted leaflet around a central axis with overlapping cusps. C, Original design created from pulling leaflets away from a central axis. D, Overlapping leaflet geometry with lines drawn from center of valve to each commissure used to redefine the free edges. E, Improved leaflet design defined by the new free edge and original equation-based curves derived from the micro-CT scan. F, Filleted leaflet geometry with smoother belly region. G, Full bioinspired trileaflet valve design with minimized commissural gaps.
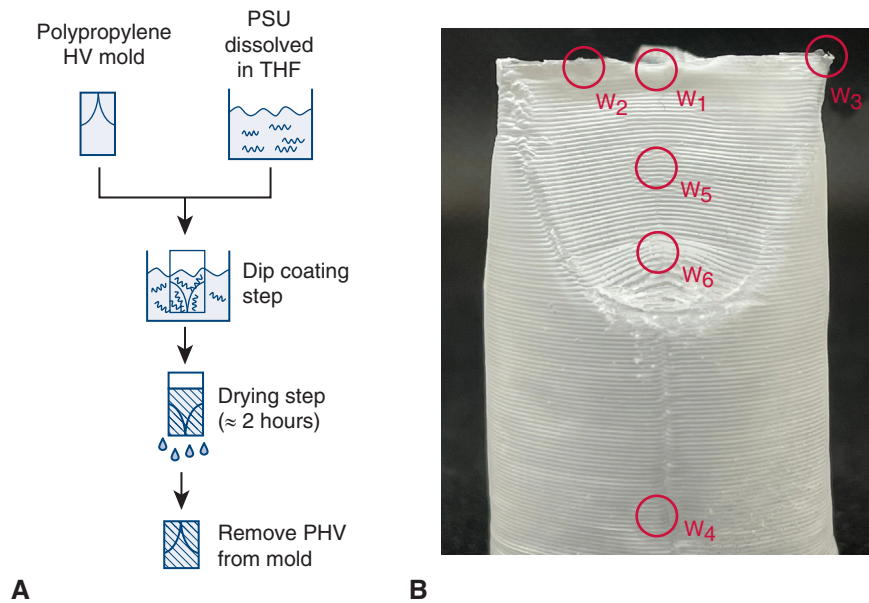
FIGURE 2. A, Schematic of the manufacturing process. The heart valve mold is 3D-printed using polypropylene and then dipped in a polysiloxane ure-thane (*PSU*) solution. After evaporation of the solvent, the polymeric heart valve (*PHV*) can be lifted off the mold. B, A PHV, with *red circles* indicating the locations where thickness was measured. *HV*, Heart valve; *THF*, tetrahydrofuran.

The Q_{RMS} is the root mean square (RMS) flow calculated over the same time period when the inflow pressure is greater than the outlet pressure,

$$Q_{RMS}\left(mL\ s^{-1}\right) = \sqrt{\frac{\int_{t_s}^{t_e} \left[Q(t)\right]^2 dt}{(t_e - t_s)}}.$$

The EOA, as defined by the ISO 5840 standard, is calculated by the equation

$$EOA\ \left(cm^2\right) = \frac{Q_{RMS}}{51.6 \times \left(\frac{Mean\ PPD}{\rho}\right)},$$

where ρ is the density of the testing fluid, in g cm^{-3}.

Finally, RF is calculated as

$$RF\ (\%) = \frac{Total\ Regurgitant\ Volume}{Forward\ Flow\ Volume} \times 100,$$

where total regurgitant volume is the sum of the closing volume and leakage volume and forward flow volume is the fluid volume moving through the valve between the start and end of forward flow.

Numerical Simulation

Commercial software LS-DYNA 2023R1 (Ansys) was used for the simulation. The ALE approach[16] coupled with an immersed solid approach as embedded in the software was used to study the FSI between the fluid flow passing through the heart valve and the deformation of the valve.
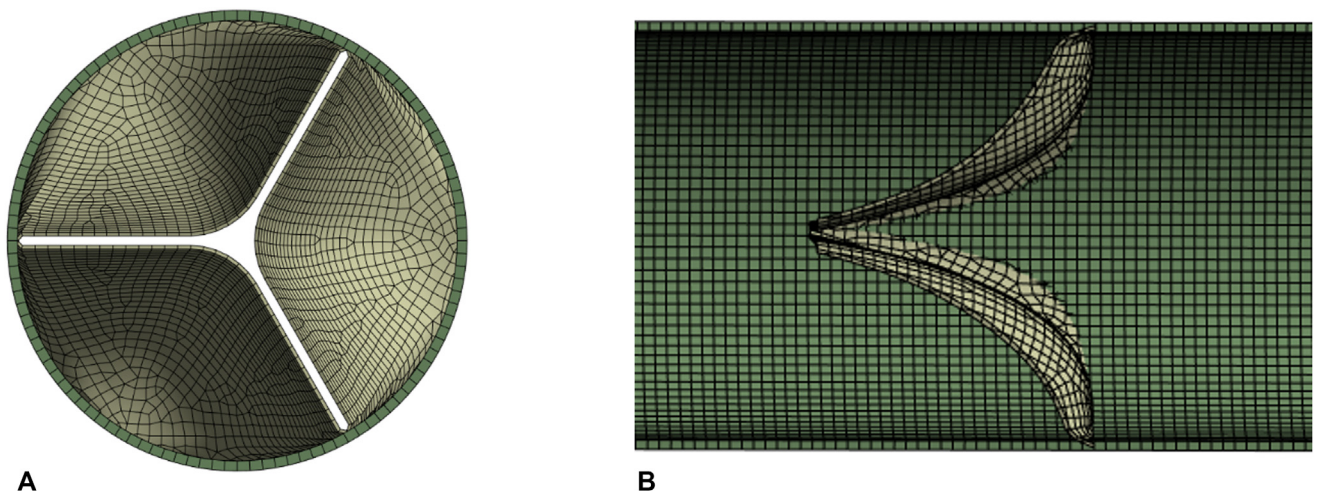

FIGURE 3. Meshed geometry of the valve (leaflets connected with the conduit) with an element size of 0.75 mm. A, Top view. B, Side view at a cross-section.
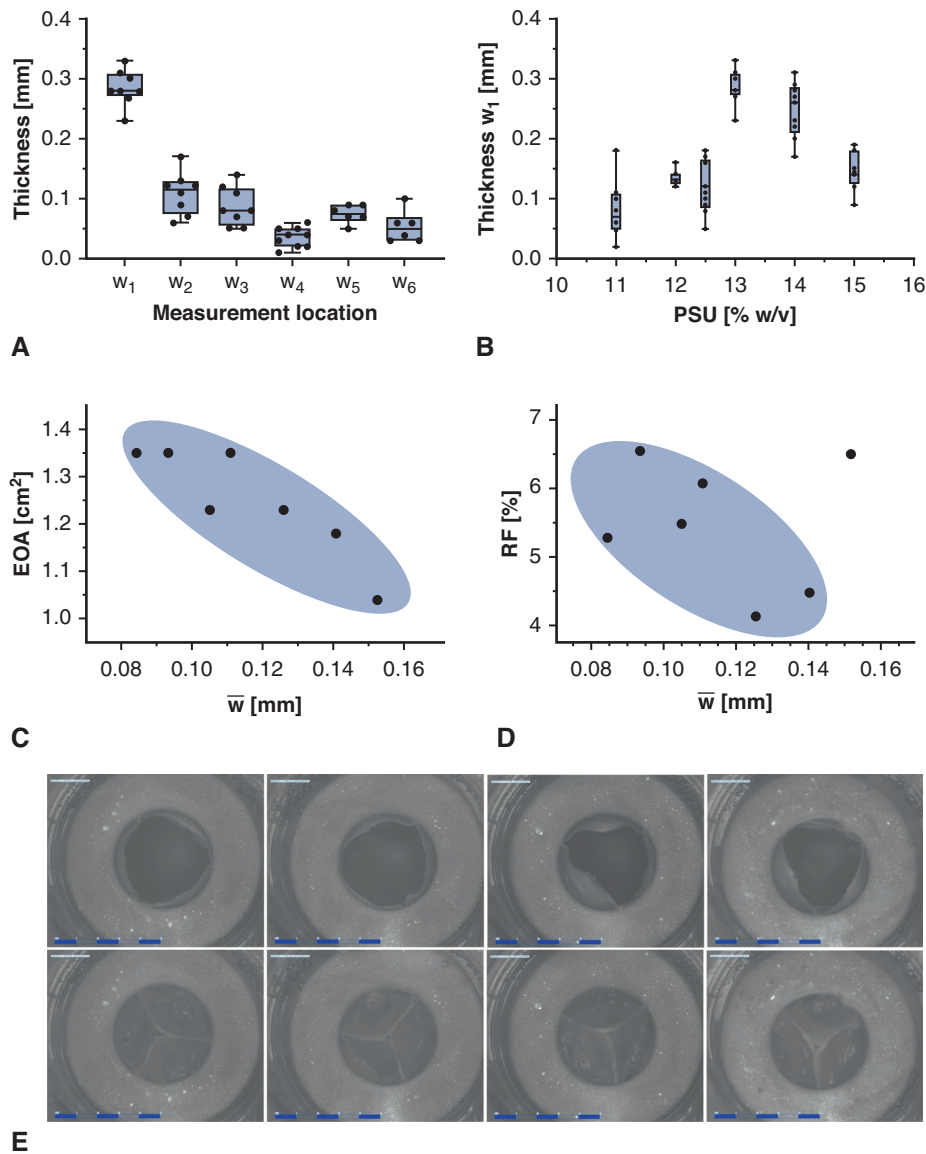
FIGURE 4. A, Thickness in different locations of the valve in polymeric heart valves (PHVs) produced using polysiloxane urethane (*PSU*) 13 w/v%. Thickness decreases from the center of the leaflet free edge to the sides (toward the commissures) and downward (toward the belly). The box spans from the first to third quartile, *whiskers* indicate the minimum-maximum range, and the line indicates the median. B, Values of w_1 for PHVs produced using different PSU concentrations. The *box* indicates the first to third quartile range, and the whiskers indicate the minimum to maximum range. C and D, The effect of thickness on the effective orifice area (*EOA*) and regurgitant fraction (*RF*); the *shaded area* in both graphs highlights the trend. E, Assessment of opening (*top*) and closing (*bottom*) performance of valves under normotensive conditions with increasing values of w_1 thickness, from left to right: 110, 150, 180, and 200 μm.

Structural deformation of the valve was simulated under dynamic pressure loading from the fluid motion, initiated by the pressure gradient obtained from the hydrodynamic test results. In this model, the fluid was assumed to be incompressible, with a density of 1000 kg m^{-3}, and to be inviscid. The conduit and leaflets were assumed to have the same density as the fluid. The material of the leaflets and the conduit were assumed to be hyperelastic, and the model parameters were adapted from Said and colleagues,[17] which are applicable to the design of vascular grafts. The Mooney–Rivlin parameters $C_{10} = -0.854$ MPa, $C_{01} = 1.82$ MPa, and $C_{11} = 0.132$ MPa were used to define the material properties.

In the simulation, the leaflets were connected to the conduit via the inter-leaflet regions. The conduit was assumed to have a thickness of 400 μm, and 4

leaflet thicknesses—110, 150, 180, and 200 μm—were studied, which covers the range tested in vitro. These thicknesses were chosen to represent the thickness at the center of the free edge (w_1) of PHV prototypes synthesized for the in vitro aspect of this study. Shell elements were used to construct the structural mesh, and an element size of 0.75 mm was applied on all the surfaces, resulting in 70,000 elements in total (mostly hexahedral) as shown in Figure 3. The base case simulation was performed using refined element sizes of 0.65 and 0.5 mm to ensure the accuracy of the results. The difference between the resulting EOA values was <1%, and thus 0.75 mm was deemed sufficient and was chosen for all future simulations to reduce computing time.

The pressure profile of the first cycle during opening from the hydrodynamic testing results was adapted and used as the boundary condition in the
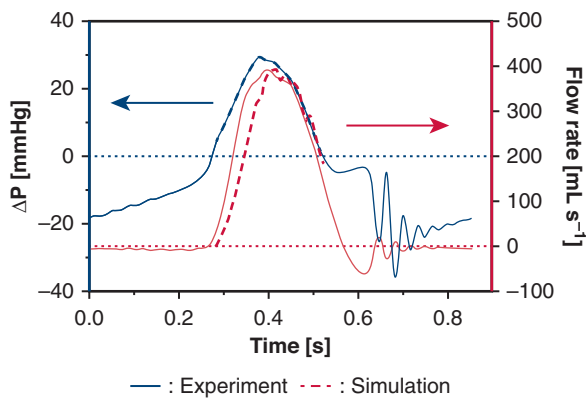
FIGURE 5. Data comparison between the experiment (*solid lines*) and the simulation (*dashed lines*) with a leaflet thickness of 110 μm for both pressure difference profile (*blue*; left *y*-axis) and flow rate (*red*; right *y*-axis). The simulation lines cover only systole. The *blue and red dotted lines* represent the 0 for the left and right axes, respectively.

simulation. This profile was used as the inlet pressure, and the outlet pressure was set to 0 to maintain the same pressure difference as in the experiment. The model was constrained using a fixed support applied to both ends of the conduit. The flow rate at the outlet was recorded at each time step. The RMS flow over the time period was used to calculate the EOA with the same equation used by the pulse duplicator system for the experimental results. The transient explicit solver was used for the structural model, and the ALE solver was used to solve the fluid flow equations. The time step is determined automatically to maintain stability with the explicit solver, and the average time-step (Δt) used was 5.1×10^{-8} seconds.

RESULTS
Hydrodynamic Testing

The thickness of the leaflet was not homogeneous and depended on the location. The center of the leaflets' free edge (w_1) (equivalent to the position of the nodule of Arantius in a native valve) proved to be the thickest, whereas the cylindrical area below the leaflet (base of the PHV prototype) was the thinnest (w_4) (Figure 4, *A*). The PSU concentration also influenced the PHV thickness. The value of w_1 increased from 81 μm for a 11 w/v% PSU solution to a maximum of approximately 250 μm for PSU concentrations of 13 w/v% and 14 w/v%. However, increasing the concentration further drastically decreased the w_1 thickness, reaching a minimum of ~150 μm (Figures 4, *B* and E1). The hydrodynamic performance of the PHVs was also correlated with the average thickness ($\overline{w}$) of the leaflets. The EOA showed an inverse correlation with the average thickness of the leaflets, with thinner valves exhibiting the largest EOAs (Figure 4, *C* and *E*). For instance, PHVs with a $\overline{w}$ of around 85 μm reached EOAs of approximately 1.35 cm^2. This value dropped to 1.05 cm^2 for leaflet thicknesses of ~150 μm. These data are supported by Figure 4, *E*, where thinner valves had larger orifices with a more circular shape and leaflets opening right up against the conduit wall. However, thinner leaflets were also correlated with

larger RF values (Figure 4, *D*). RF values ranged from a minimum of approximately 4% for the thickest PHV to a maximum of 6.5%.

Numerical Simulation

The PPD profile from the in vitro testing results was used as the simulation pressure input, as shown in blue in Figure 5. The resulting flow rate obtained as the simulation output was compared against the experimental results, presented in the same figure and shown in red. The maximum flow rates from the experiment and the simulation were well matched despite the setup differences, which are explained in detail in the Discussion section.

The displacement and stress distribution profiles for the valves with leaflet thicknesses of 110, 150, 180, and 200 μm are compared in Figure 6. In general, valves with thinner leaflets performed better in terms of snap-through behavior. Snap-through, defined previously,[13] describes a valve whose leaflets can bend against the natural curvature during systole to allow for maximum opening. As leaflet thickness increased, both the maximum displacement of the leaflets and the EOA decreased (Figure 7), demonstrating less mobility. This pattern was consistent with experimental results. However, the stress distribution profiles were not significantly different among various thicknesses, as shown in Figure 6. The maximum stress varied from 1.3 MPa to 1.7 MPa, which was observed around the commissures and at the edges where the leaflets and the conduits were connected.

DISCUSSION

The ultimate goal of this work was to design PHV replacements with enhanced performance and durability. The performance of our design was tested by both in vitro and in silico studies. The experimental and simulation results showed similar correlations between leaflet thickness and valve systolic function despite some differences in the two approaches. These results show promise for the combined in vitro–in silico approach, further highlighting computational modeling as a strong tool for assessing valve function and its role in this workflow for streamlining valve development and testing. See Figure 8 for a graphical abstract of the study.

To test the effect of leaflet thickness, uniform thicknesses were used in the simulation. However, PHV prototypes showed a gradient in thickness because of the drying process, as shown in Figure 4, *A*. Drying the PHVs with the leaflets inverted caused an accumulation of material in the central part of the leaflet free edge, where w_1 is measured, whereas the base of the valve was thinner. The nonuniformity of the thickness across each leaflet attempted to resemble the heterogeneity of native leaflets thickness. Moreover, although the discrepancy in thickness was minimal in some cases, reducing intersample variation in
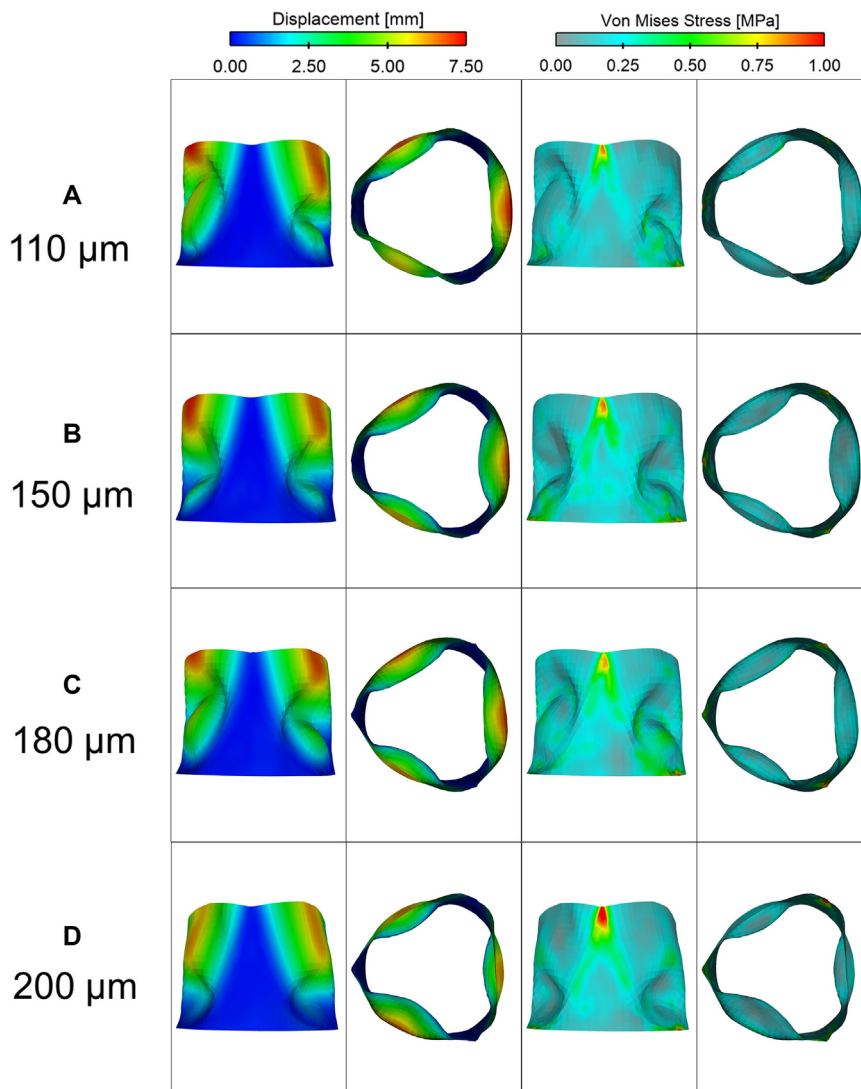
FIGURE 6. Displacement (*left*) and stress distribution (*right*) for fully opened valves from side and top views with different leaflet thicknesses: 110 μm (A), 150 μm (B), 180 μm (C), and 200 μm (D).

thickness using a manual dip-coating procedure proved challenging. Thus, there is a need for further optimization of the fabrication process, with automation applied wherever possible for improved reproducibility.

The effect of thickness on the PHVs' performance was investigated. Both EOA and RF increased with thinner leaflets. Thinner leaflets offer less resistance during systole compared with thicker leaflets, resulting in a larger EOA. This is because thinner leaflets are characterized by a lower flexural rigidity, which is directly proportional to the thickness.[18] Flexural rigidity is a measurement of how much resistance to bending a component would oppose, with lower values indicating more flexible objects. As such, thin valves usually have wider orifices. This explanation is also supported by the simulation results, with thicker valves exhibiting smaller displacement and higher stresses during opening. Similarly, valves characterized by thin leaflets

show higher RFs, most likely due to a combination of causes arising from reduced thickness, such as decreased flexural rigidity and increased displacement during systole. In fact, with greater displacement, the leaflets take longer to return to a closed position during diastole. This leaves the valve open for longer during backflow and increases regurgitation slightly. The hydrodynamic results obtained for all thicknesses are compliant with the ISO 5840-2, with all RF values <10% and all EOA values >0.85 cm^2 (requirements for a 19-mm valve). In the absence of an 18 mm standard, the 19 mm value was used to avoid overestimating hydrodynamic performance. These outcomes are also comparable with clinically used bioprosthetic valves tested in the pulmonary position of a pulse duplicator system.[19] The EOA of 21-mm diameter bioprosthetic valves and polyurethane prototypes from this study were both approximately 60% greater than that outlined by the standard, 1.05 cm^2
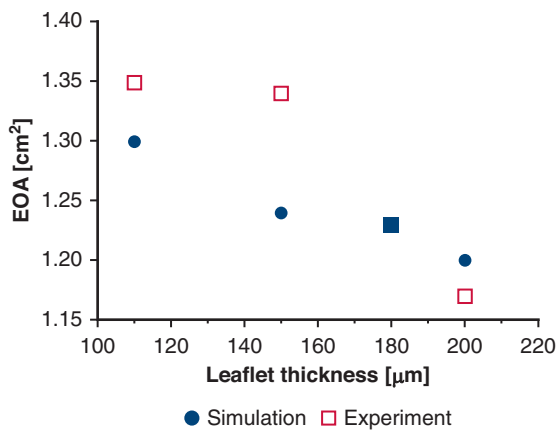
FIGURE 7. Comparison of the effect of leaflet thickness (w$_1$) on effective orifice area between the simulation and experimental results. Note that the data points for simulation and experiment overlap for 180 μm. *EOA*, Effective orifice area.

(21 mm diameter) and 0.85 cm^2 (19 mm diameter), respectively. Because this comparison is an underestimation of the hydrodynamic performance, it is further hypothesized that polyurethane valves may perform on par with or better than current treatments.

Limitations and Future Studies

It must be noted that the results shown in Figure 4, *C* and *D* depict the correlation of the average thickness to EOA and RF, respectively. Nevertheless, w$_1$ had a greater impact on hydrodynamic performance compared with other thickness values (Figure E2). This is possibly due to the discrepancy between w$_1$ and the rest of the values (eg, from the 275 μm of w$_1$ to approximately 100 μm for w$_2$ in 13 w/v % valves). The presence of outliers then can be explained by the heterogeneous distribution of thickness along different areas of the leaflet. Although these values (ie,
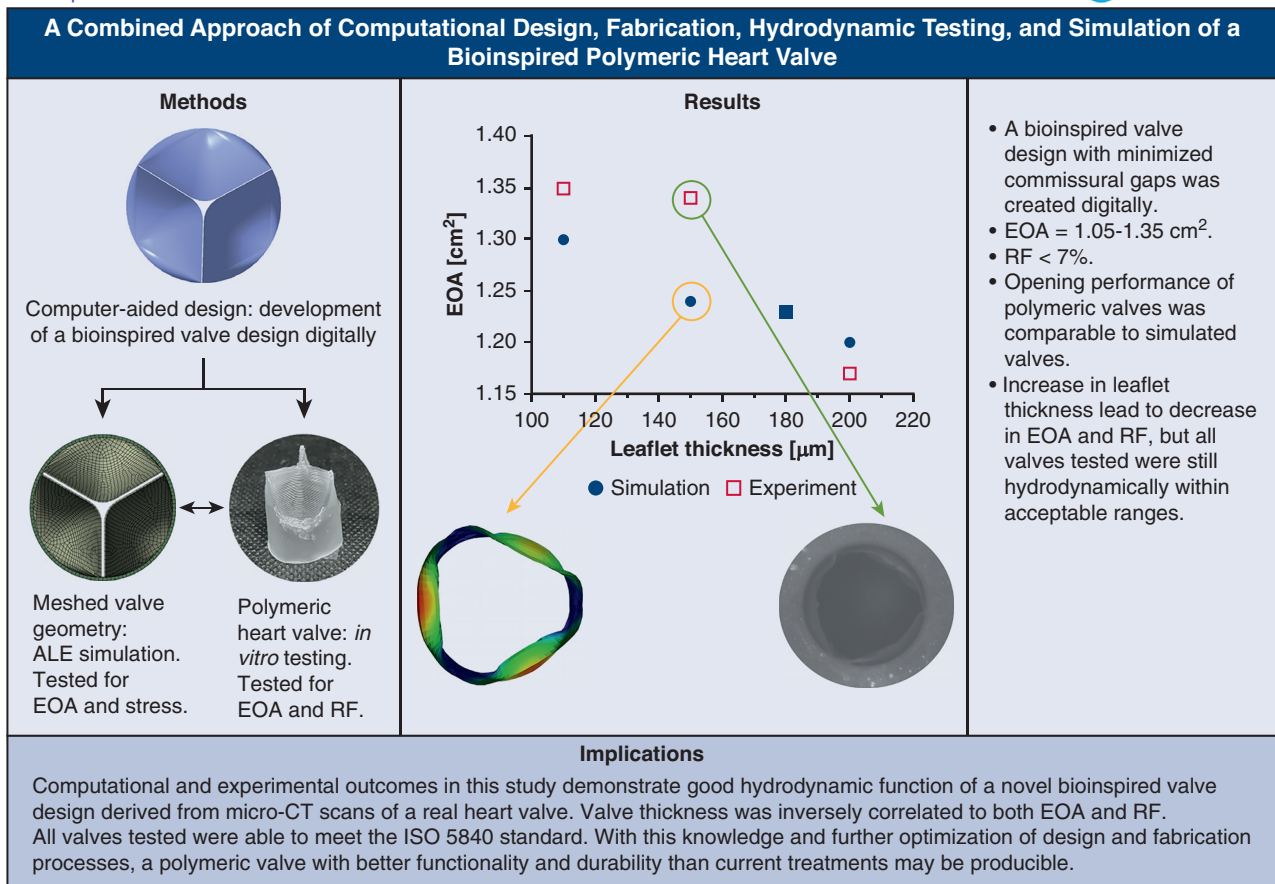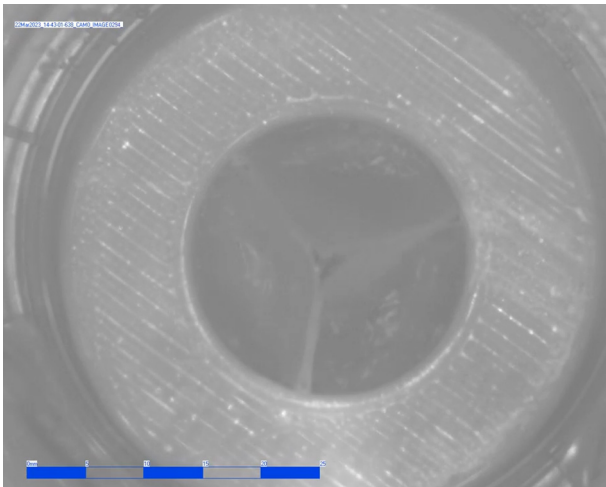

FIGURE 8. Graphical abstract depicting study workflow, results, and implications. *EOA*, Effective orifice area; *RF*, regurgitant fraction; *ALE*, arbitrary Lagrangian-Eulerian; *CT*, computed tomography.

VIDEO 1. Polymeric heart valve hydrodynamic test in pulse duplicator. Video available at: https://www.jtcvs.org/article/S2666-2736(23)00184-5/fulltext.

w_2, w_3, etc.) do not show a direct correlation with either EOA or RF, they still may have significance for the overall performance of the PHV. The nonhomogeneous thickness in fabricated samples is possibly the reason why the EOA values obtained differ slightly from those obtained via simulation. For the in silico studies, the thickness is set to a constant value (ie, w_1) throughout the leaflets, which is a significant assumption that may lead to differences with the PHV prototypes. Furthermore, PHVs were glued to rigid conduits that drastically narrowed the flow area from the 50-mm valve exchange chamber belonging to the pulse duplicator upstream to 18 mm (conduit diameter). In simulation, this sudden change in diameter was not present, as the upstream and downstream fluid domain were set to match the valve diameter, and the valve was placed in a hyperelastic conduit rather than a rigid holder. Therefore, further studies are needed to understand the impact of the leaflet thickness in different areas on hydrodynamic performance.

Furthermore, although a bioinspired design was explored, the PHVs produced did not replicate the mechanical anisotropic behavior of native valves. This may affect hydrodynamic performance and will be investigated in studies involving leaflet reinforcements. Future studies also will include optimizing the thickness distribution to better mimic that of native valves, incorporating valved conduits with sinuses, comparing hydrodynamic performance with PHVs constructed from different polymers, and in vivo analysis in sheep, including evaluation of thrombogenicity and calcification. Further assessment of material fracture, fatigue, and durability will be conducted both in silico and in vitro to evaluate the clinical potential of the valve.

In the simulation, an ALE plus immersed solid approach was applied to study the interaction between the valve and the fluid passing th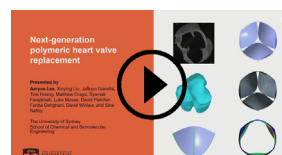rough the system. This approach used an inviscid fluid, and fluid boundary layer effects, such as drag and recirculation, were not considered, a limitation of this work. Further investigation will be needed to test these effects and whether they have significant impact on this dynamic system by involving a viscous fluid. Only the systolic behavior of the valve was simulated in this study, owing to limitations in the current workflow. Due to the computationally expensive nature of the explicit time integration scheme, only the first cycle was used, instead of the total 10 cycles from the hydrodynamic testing results. In future studies, a full FSI simulation, which includes the fluid boundary layer effect, should be investigated and compared with the ALE approach.

CONCLUSIONS

This work presents a coupled workflow for evaluating the performance of a bioinspired valve design with improved free edge geometry. Leaflets demonstrated good mobility; however, limitations in the manual fabrication process prevented fine control over material thickness. Resulting PHV prototypes showed EOAs and RFs ranging from 1.05 cm^2 to 1.35 cm^2 and from 4% to 6.5%, respectively, and were hydrodynamically acceptable based on ISO 5840-2. In general, valves with thinner leaflets resulted in larger orifice areas but also led to slightly more regurgitation. Computationally, the same valve counterparts exhibited EOAs of 1.2 to 1.3 cm^2, a comparable range as in the in vitro prototypes. In silico studies also illustrated snap-through of valves with thinner leaflets and showed the stress distribution profiles were not significantly impacted by leaflet thickness. Further investigation is needed to study the effect of thickness on durability, suture retention, and tests with a flexible conduit.[20] Future work will involve optimization of the valve design and fabrication process, as well as a full FSI analysis with simulation of the diastolic performance of valves.

Webcast

You can watch a Webcast of this AATS meeting presentation by going to: https://www.aats.org/resources/next-generation-bioinspired-polymeric-pulmonary-heart-valve-replacements.

Conflict of Interest Statement
The authors report no conflicts of interest.

References

1. Yacoub MH, Takkenberg JJ. Will heart valve tissue engineering change the world? *Nat Clin Pract Cardiovasc Med*. 2005;2:60-1.
2. Crago M, Winlaw DS, Farajikhah S, Dehghani F, Naficy S. Pediatric pulmonary valve replacements: clinical challenges and emerging technologies. *Bioeng Transl Med*. 2023;8:e10501.
3. Applegate PM, Boyd WD, Applegate II RL, Liu H. Is it the time to reconsider the choice of valves for cardiac surgery: mechanical or bioprosthetic? *J Biomed Res*. 2017;31:373-6.
4. Cote N, Pibarot P, Clavel MA. Incidence, risk factors, clinical impact, and management of bioprosthesis structural valve degeneration. *Curr Opin Cardiol*. 2017; 32:123-9.
5. Hammermeister KE, Sethi GK, Henderson WG, Oprian C, Kim T, Rahimtoola S. A comparison of outcomes in men 11 years after heart-valve replacement with a mechanical valve or bioprosthesis. Veterans Affairs Cooperative Study on Valvular Heart Disease. *N Engl J Med*. 1993;328:1289-96.
6. Kostyunin AE, Yuzhalin AE, Rezvova MA, Ovcharenko EA, Glushkova TV, Kutikhin AG. Degeneration of bioprosthetic heart valves: Update 2020. *J Am Heart Assoc*. 2020;9:e018506.
7. O'Brien MF, Stafford EG, Gardner MA, Pohlner PG, Tesar PJ, Cochrane AD, et al. Allograft aortic valve replacement: long-term follow-up. *Ann Thorac Surg*. 1995;60:S65-70.
8. Tillquist MN, Maddox TM. Cardiac crossroads: deciding between mechanical or bioprosthetic heart valve replacement. *Patient Prefer Adherence*. 2011;5:91-9.
9. Vongpatanasin W, Hillis LD, Lange RA. Prosthetic heart valves. *N Engl J Med*. 1996;335:407-16.
10. Yacoub M, Rasmi NR, Sundt TM, Lund O, Boyland E, Radley-Smith R, et al. Fourteen-year experience with homovital homografts for aortic valve replacement. *J Thorac Cardiovasc Surg*. 1995;110:186-93; discussion 193-4.
11. Saxena A, Salve GG, Betts K, Arora N, Cole AD, Sholler GF, et al. Outcomes following heterotopic placement of right ventricle to pulmonary artery conduits. *World J Pediatr Congenit Heart Surg*. 2021;12:220-9.
12. Kereiakes DJ, Answini GA, Yakubov SJ, Rai B, Smith JM, Duff S, et al. Preliminary evaluation of a novel polymeric valve following surgical implantation for Symptomatic aortic valve disease. *JACC Cardiovasc Interv*. 2021;14:2754-6.
13. Lee A, Farajikhah S, Crago M, Mosse L, Fletcher DF, Dehghani F, et al. From scan to simulation-A novel workflow for developing bioinspired heart valves. *J Biomech Eng*. 2023;145:055001.
14. Oveissi F, Naficy S, Lee A, Winlaw DS, Dehghani F. Materials and manufacturing perspectives in engineering heart valves: a review. *Materials Today Bio*. 2020;5:100038.
15. Singh SK, Kachel M, Castillero E, Xue Y, Kalfa D, Ferrari G, et al. Polymeric prosthetic heart valves: a review of current technologies and future directions. *Front Cardiovasc Med*. 2023;10:1137827.
16. Donea J, Huerta A, Ponthot J-P, Rodríguez-Ferran A. *Arbitrary Lagrangian–Eulerian Methods*. Encyclopedia of Computational Mechanics; 2004.
17. Said AA, Carlos DP, Manuel FV. Mechanical assessment and hyperelastic modeling of polyurethanes for the Early Stages of vascular Graft design. *Materials (Basel)*. 2020;13:4973.
18. Johnson EL, Rajanna MR, Yang C-H, Hsu M-C. Effects of membrane and flexural stiffnesses on aortic valve dynamics: identifying the mechanics of leaflet flutter in thinner biological tissues. *Forces Mech*. 2022;6:100053.
19. Pragt H, van Melle JP, Verkerke GJ, Mariani MA, Ebels T. Pulmonary versus aortic pressure behavior of a bovine pericardial valve. *J Thorac Cardiovasc Surg*. 2020;159:1051-9.e1051.
20. Bernacca GM, Mackay TG, Gulbransen MJ, Donn AW, Wheatley DJ. Polyurethane heart valve durability: effects of leaflet thickness and material. *Int J Artif Organs*. 1997;20:327-31.
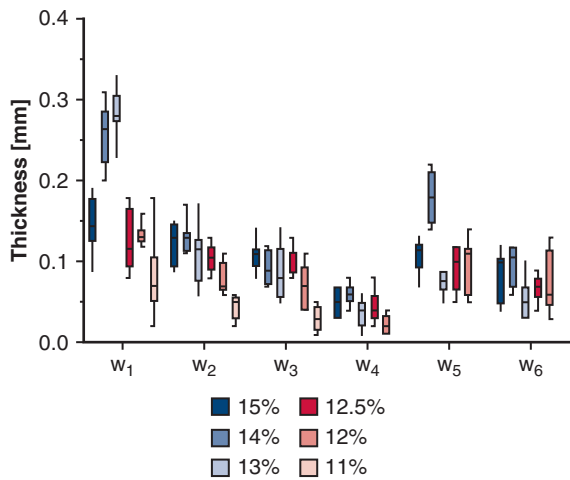
FIGURE E1. Dispersion of thickness at different points of the leaflet for all PSU concentrations tested. Note how the thickness follows a somewhat similar trend for all concentrations, being highest at the center of the leaflet free edge (w1) and thinnest at the base below the valve (w4). The thickness at w5 for the 14 w/v% PSU valves does not follow the trend and thus will be further investigated in future experiments. N.B. The process of dip coating produces 100% PSU layers after solvent evaporation (hence, material properties do not change). The thickness of this layer depends mainly on the viscosity (μ) and density (ρ) of the dipping solution, which depend on the concentration of PSU.
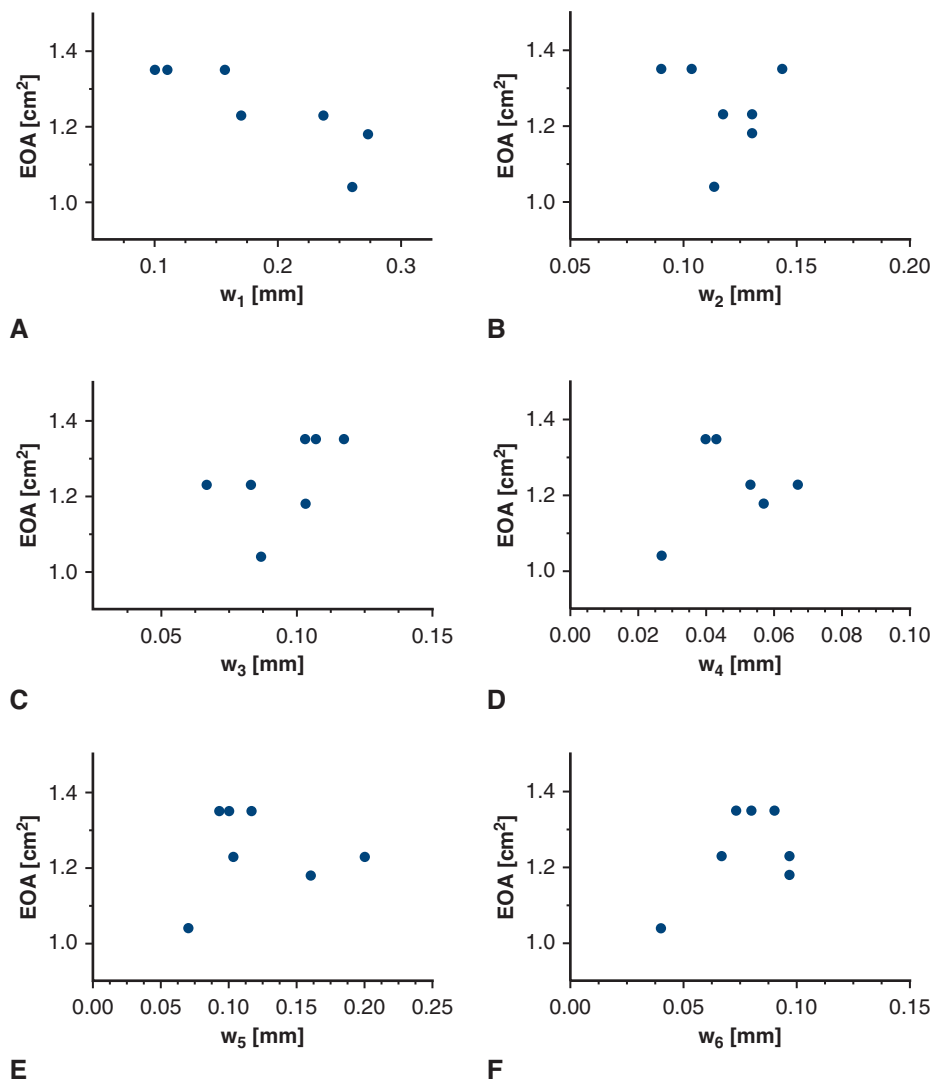
FIGURE E2. Effect of thickness of different locations on the leaflet—w1 (A), w2 (B), w3 (C), w4 (D), w5 (E), and w6 (F)—on the effective orifice area (*EOA*). Note that only w1 has a correlation between thickness and EOA (with EOA decreasing with increasing thickness). For all other values of thickness, there is no clear trend. This highlights the sensitivity of hydrodynamic performance on w1.